Approximation of electronic term of diatomic molecule by the Morse function. The role of anharmonicity

R.E. Asfin*, G.S. Denisov

Department of Physics, Saint Petersburg State University, 7/9 Universitetskaya Nab., 199034 Saint Petersburg, Russian Federation

*Corresponding author: R.Asfin@spbu.ru

Abstract

This article presents an extension of the report made at the 2nd International Symposium "Non-Covalent Interactions" 10/14/22 in Moscow. That report outlined the basic principles of modeling the potential function of diatomic molecules using the Morse potential. Based on the published results of high-level quantum-chemical calculations, as well as the experimental spectroscopic measurements of the vibrational structure of electronic transitions, potential curves for several molecules were constructed and their approximations were carried out using the Morse formula. The possibilities of using the Morse formula as the simplest anharmonic approximation for describing the features of the shape of potential curves and their vibrational structure of a real molecule are evaluated. A perspective is outlined for studying the bond character in van der Waals diatomic molecules according to the shape and features of anharmonicity function.

Keywords: Morse function, Anharmonicity, Diatomic molecules, Electronic terms, Vibration structure, Approximation

1. Introduction

Despite the rough approximation, the high popularity of the three-parameter Morse function is beyond doubt, mainly due to the possibility of analytically solving the Schrödinger equation with this potential in a good approximation. Applications of the Morse approximation are rapidly growing in fundamental and applied physical chemistry, in particular, in the study of intermolecular interactions, adsorption, impurity centers in crystals, elementary reaction kinetics, etc. Therefore, recent publications devoted to the development of Morse's ideology and methods of its practical application are relevant.

In the current communication the main attention is focused on the development of the original results of the authors' recent work on the features of the Morse approximation [1–3]. They include the existence of two independent interpretations M1 and M2 of the solution of the Schrödinger equation for an alternative approximations of the potential function of the molecule $U(r)$, the introduction of the empirical anharmonicity function $\omega_e x(v)$, which

characterizes the anharmonicity of the potential well in the vicinity of the vibrational quantum number v, the development of the approach for estimating the deviations of the models M1 and M2 from the real term $U(r)$. To estimate the shape of the contour of the models and the structure of their vibrational spectra, the approach involves the joint utilization of the Birge-Sponer plot and the difference $U(r)$ and model functions, $\delta(r) = U(r) - M(r)$. A primary empirical classification of electronic terms based on the shape of the anharmonicity function $\omega_e x(v)$ and deviations $\delta(r)$ of M1 and M2 from the true potential is proposed. The specific features of these functions for van der Waals molecules are described.

2. Approach

The Morse formula used to approximate the real electronic term of a diatomic molecule has the form [4]:

$$M(r) = D_e\left[1 - \exp\left(-a(r - r_e)\right)\right]^2 \qquad (1),$$

the eigenvalues (vibrational energies) of this potential are approximately (series is limited by two terms):

$$E(v)/hc = G(v) = \omega_e(v + ½) - \omega_e x_e(v + ½)^2 \qquad v = 0,1,2 \ldots v_m \qquad (2),$$

where ω_e, harmonic frequency, cm^{-1}, and $\omega_e x_e$, anharmonicity, cm^{-1}, are parameters which can be calculated from two experimental vibrational frequencies $\omega(0-1)$ and $\omega(0-2)$, and v_m is maximum vibrational quantum number, which defines the bond energy D_e. Coefficients in (2) expressed in terms of parameters of (1) and the reduced mass μ, are:

$$\omega_e = a(2D_e/\mu)^{½} \qquad (3a), \qquad \omega_e x_e = a^2/2\mu \qquad (3b).$$

Excluding "a" from (3a) and (3b), one obtains the expression for the bond energy

$$D_e = \omega_e^2/4\omega_e x_e \qquad (4)$$

This formula is exact only if (2) is strictly correct, and the positions of the vibrational levels are described by a single anharmonicity coefficient $\omega_e x_e$, then M1=M2. In reality, the inaccuracy of (4) always complicates the description of the system.

It was shown in [1] that when approximating the real term $U(r)$ by the Morse function, the exponent "a" in (1) can be expressed in terms of experimentally observed parameters in two ways, using either (3a) or (3b). The resulting solutions M1 and M2 are not identical and can be applied in different situations, see [3]; an interesting example of the rarely used M2 has recently appeared [5]. Such ambiguity is inherent in Morse's formula from the very beginning, it is explained by the impossibility of reaching his goal – to introduce into the harmonic potential two independent parameters, the asymptote D_e and the anharmonicity x_e (or $\omega_e x_e$) – using only one parameter. The coefficient "a" contains both of these parameters, but they cannot vary simultaneously. Equation (3a) defines D_e, but then one needs to fix $\omega_e x_e$, and this yields M1; equation (3b) gives $\omega_e x_e$, but in this case, one needs to know D_e, and this gives M2. For

M1, the D_e value is calculated by a distant extrapolation based on the anharmonicity of the lowest vibrational levels, and for M2, for a given D_e and ω_e, the dimensionless anharmonicity x_e is calculated from (4) as $x_e{}' = \omega_e/4D_e$ (we will mark the parameters of Morse models with primes).

It can be suggested that the main Morse's goal was to determine the binding energy, and the use of equation (4) was a necessary intermediate step. The possibility of an alternative solution for M2 follows from Morse's construction, but was not explicitly mentioned by him.

2.1. Quantitative characteristics of Morse approximations

Figure 1 shows the term of the ground state $X\ {}^1\Sigma_g^+$ of the F_2 molecule constructed from high quality calculated data [6]. Based on the same data, approximations of this term by the Morse formula M1 (red line) and M2 (blue line) were build. The energy of the M1 term rises above $U(r)$ with acceleration, since the real vibrational levels converge faster than it occurs when anharmonicity $\omega_e x_e$ is constant. Therefore, the asymptote for M1 is much higher than that for the real term, and several additional fictitious vibrational levels appear between them. Curve M2 has an asymptote equal to the experimental value D_e, and the anharmonicity $\omega_e x_e'$ must be greater than $\omega_e x_e$, but since ω_e is fixed, $\omega_e x_e'$ increases at the expense of x_e. The density of vibrational levels increases, as well as the width of the potential well, so the curve $U(r)$ runs between M1 and M2 without crossing. The distance between $U(r)$ and M2 increases at first,

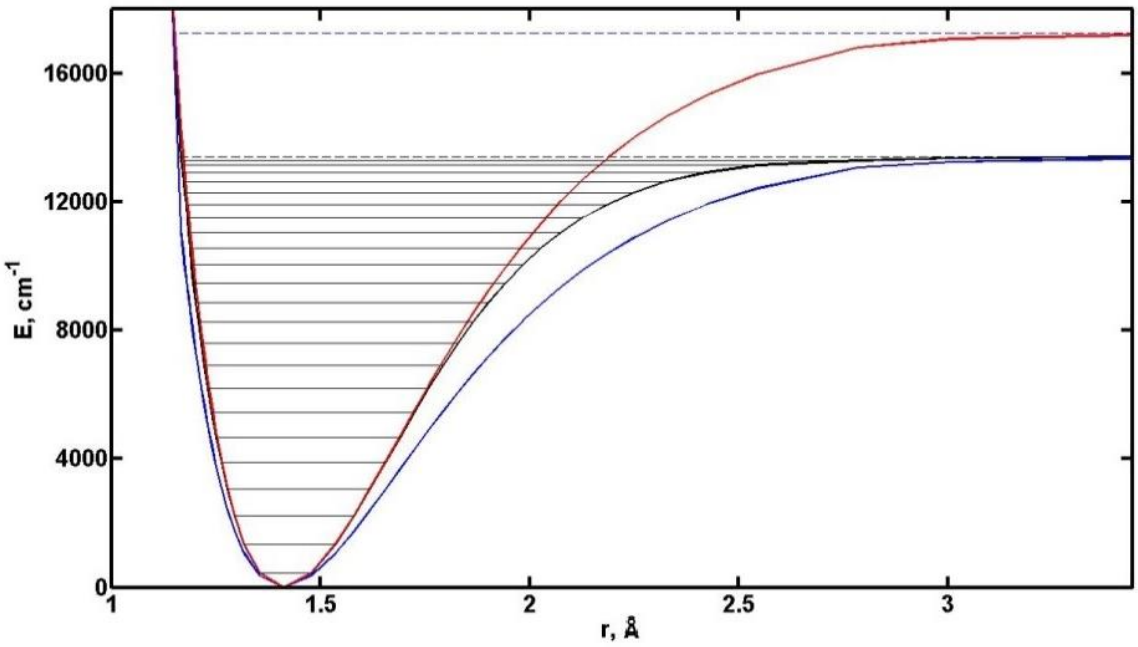

Figure 1. The term $X\ {}^1\Sigma_g^+$ of the F_2 molecule (black line) according to [6] and its Morse approximations M1 (red) and M2 (blue).

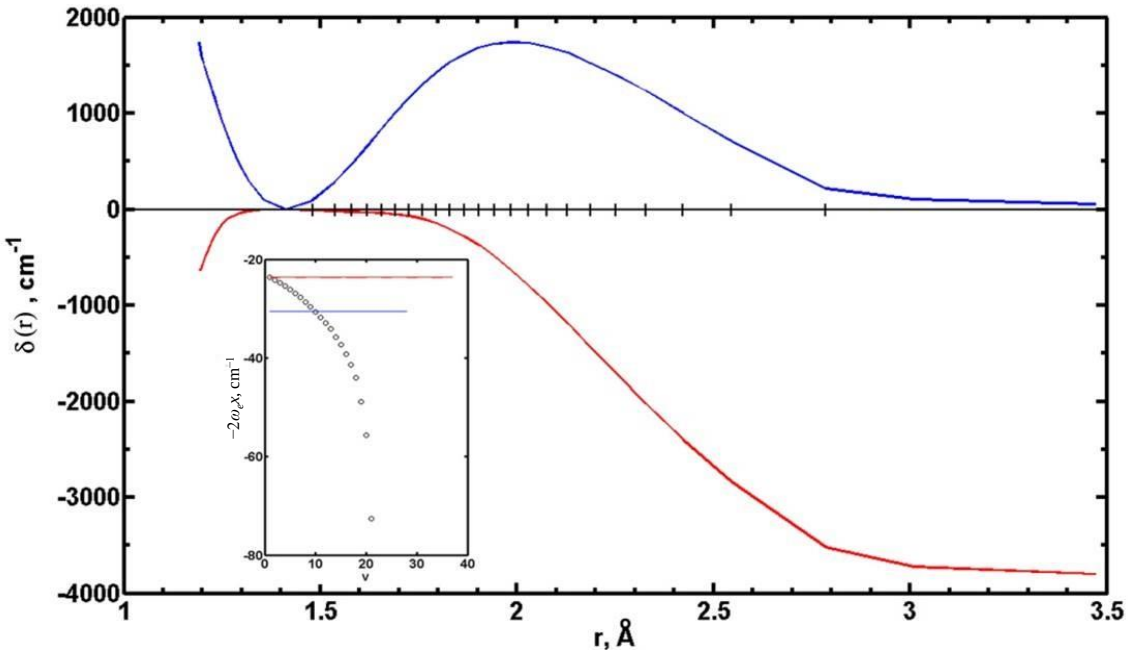

Figure 2. Deviations of M1 (red line) and M2 (blue) from the term $X\ ^1\Sigma_g^+$ of the F_2 molecule according to [6]. Vertical dashes on the abscissa axis $\delta(r)$ are the values of the outer classical turning points r_2 of vibrational levels (region of maximum of probability density function). In the inset, the anharmonicity $-2\omega_e x(v)$ is shown (points), with parallel lines illustrating constant values of anharmonicity $-2\omega_e x_e$ for M1 (red) and $-2\omega_e x'_e$ for M2 (blue)

passes through a maximum and then decreases to zero when $U(r)$ and M2 reach the common asymptote $D'_e = D_e$. Due to the increased anharmonicity in the approximation M2, several fictitious terms also appear adjacent to the asymptote.

A clear and comprehensive characteristic of approximation of the term $U(r)$ is the difference – the deviation function $\delta(r) \equiv U(r) - M(r)$ for M1 and M2 [3]. Fig.2 shows plots of these data for the F_2 molecule, built according to the results from [6]. In the lower part of the potential well (~40% of its depth, up to v=7), the deviation of M1 with an excess no more than 100 cm^{-1}, is close to $U(r)$. The deviation increases monotonously to the limit ~4000 cm^{-1}, which is 35% higher than the calculated value of D_e = 13375 cm^{-1}. For M2, $\delta(r)$ has a domed shape with maximum 1800 cm^{-1} in the upper part of the potential well. In the main part of the well (up to ~90%, $v = 17$) the M1 model alters the shape of the term to a lesser extent than M2.

The distortion of the vibrational structure at approximation is illustrated in the Birge-Sponer coordinates (Fig. 3), here $\omega(v) \equiv \Delta_1 G(v) = G(v+1) - G(v)$ are vibrational quanta [1]. Experimental frequencies constitute a curve (Birge-Sponer plot, points), extrapolation of which to the abscissa axis closes the figure with area D_0 (the sum of all vibrational quanta) (D_e=D_0 + $G(0)$, [7]). The straight line M1 (red) is drawn through the points v = 1 and 2, which determine the anharmonicity $\omega_e x_e$, let's call it the Birge-Sponer straight line. It shows the positions of

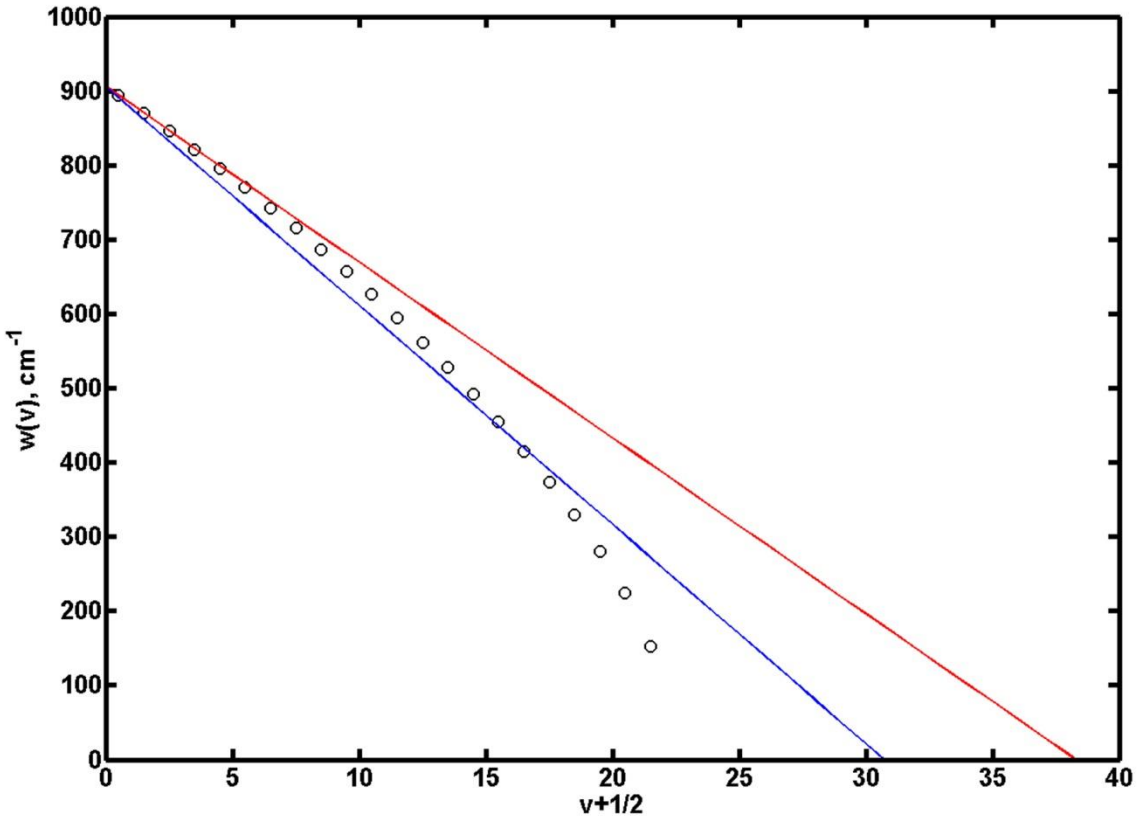

Figure 3. Birge-Sponer plot (points) for the term $X\ ^1\Sigma_g^+$ of the F_2 molecule according to [6] and its Morse approximations M1 (red straight line) and M2 (blue straight line).

vibrational frequencies in M1. The values of frequencies are overestimated, in the lower part of the term the deviation is small and monotonously increases with increasing v. The slope of the straight line M2 (blue) is determined by the value $\omega_e x_e'$, while the area under the straight line is equal to D_0. Here the deviation is underestimated and is large already near the bottom of the potential well, then it passes through a minimum and changes sign. The points on the straight lines are not shown; they correspond to half-integer abscissas.

It is useful to introduce the empirical anharmonicity function $\omega_e x(v)$ [1]:

$$\Delta_2 G(v) = w(v+1) - w(v) \equiv -2\omega_e x(v), \qquad (5)$$

which more accurately represents the frequency distortions in M1 and M2 models and serves as a characteristic of the vibrational structure of the term $U(r)$. The points in the inset Fig.2 show the shape of this function. For the ground term of fluorine, it monotonously increases with acceleration. The horizontal lines show the values of anharmonicity for M1 (red) and M2 (blue). The length of the lines characterizes the total number of levels, including fictitious ones. Note that the value of $\omega_e x(v)$ is determined by the energy of three levels v, $v+1$, $v+2$, with the second of them used as the abscissa. For the Morse potential, anharmonicity function is constant $-2\omega_e x_e$ for M1 and $-2\omega_e x_e'$ for M2.

3. Results

For a number of electronic terms of diatomic molecules, the model potential functions M1 and M2, as well as deviations δ(r) are constructed according to the literature data. The later characterizes the changes in the real term contour upon approximation. Birge-Sponer plots $w(v)$ (vibrational frequencies *vs* vibrational quantum number) and functions $\omega_e x(v)$ (see eq. (5)) characterizing the change in frequencies are built. The results allow for preliminarily classification of the real terms of diatomic molecules with a valence bond into three groups: simple terms with a monotonously increasing anharmonicity, terms with anomalies in the lower part of the potential well, and terms with anomalies near the asymptote due to a change in the type of interatomic interaction at large distances. A special class is comprised by the fourth group, the group of van der Waals molecules, in which the anharmonicity monotonously decreases with v. In this case attention is focused directly on the experimental or calculated vibrational spectrum of a diatomic molecule, whereas Morse modeling is not necessary.

3.1. Simple terms

The term of the ground state $X\ ^1\Sigma_g^+$ of the F_2 molecule, described in detail above, belongs to this group. It can be added, that the repulsion branch of M1 in Fig. 1 looks unexpected, it is located above the original term, but almost merges with it at the edge of the continuous spectrum. This feature, which was confirmed later by another calculation, still requires additional analysis. In general, the description of the behavior of the repulsive branch of models M1 and M2 on the basis of existing materials encounters difficulties, it is not possible to formulate simple empirical patterns. It seems natural that they should run below the $U(r)$ curve, since, according to the Morse asymptotics, they must intersect the ordinate in the region of the continuous spectrum, and for the most terms the deviations $\delta(r)$ are really positive. However, there are also examples of model terms, running above $U(r)$, - for O_2 the deviations $\delta(r)$ are negative for M1 and M2, for F_2 only for M1. We tend to think that these data are heavily hampered by systematic errors in the calculations of the repulsion potential, but this does not change the main results and conclusions.

The main features of simple terms are monotonous increase of anharmonicity $\omega_e x(v)$ and of deviation $\delta(r)$ for M1 and the appearance of a smooth dome in $\delta(r)$ for M2. Besides F_2 they are characteristic for the free radical term $X\ ^2\Sigma^+$ BeH and a few other terms that form the first group. Similar features are also observed in the major part of the potential curve for terms assigned to the third group, which exhibit anomalies in the region of the last vibrational levels near the asymptote, for example, Li_2 and B_2.

3.2. Peculiarities in the lower part of potential well

The terms with anomalies in the lower part of the potential well (the second group) include the ground term $X\ ^1\Sigma_g^+$ of hydrogen H_2, historically the first example (in 1939) of detecting deviations occurring in the Morse approximation. In Herzberg's book [8], Figure 48 shows this

deviation with a dotted line, with intersection between the terms $U(r)$ and M2. Deviations from the Birge-Sponer straight line are barely noticeable (Fig. 10 in [9]). The narrowing of the H_2 term also is manifested in an increasing distance between the vibrational levels $v = 0 \div 6$, that is, in a decrease of anharmonicity, and non-monotonous function $\omega_e x(v)$. These changes are shown in Fig. 4, which was built using data from [10]. Additional extrema appear on the curves $\delta(r)$ for M1 and M2, and the curve for M2 crosses the abscissa, where $\delta(r)$=0. The intersection between the terms is shown in the inset A. In [1], we called this anomaly the Herzberg Anomaly, HA. It is noteworthy that 20 years later Herzberg and Howe [11], discussing the experimental dependencies $\Delta_1 G(v)$ and $\Delta_2 G(v)$ in the spectrum of H_2 (the latter almost exactly coincides with our inset B), in conclusion especially noted this anomaly as deserving the attention of theorists.

The similar anomaly with the intersection of terms is also observed in the ground term of the Be_2 molecule [12], where the deviation has a different sign, i.e. the potential well in the lower part is broadened compared to the Morse function (see Fig.3 in [12]). In this case the vibrational levels are closer, and the function $\omega_e x(v)$ has a minimum (see Fig.4 in [1]).

For several terms studied, the anharmonicity in the lower part of the well grows non-

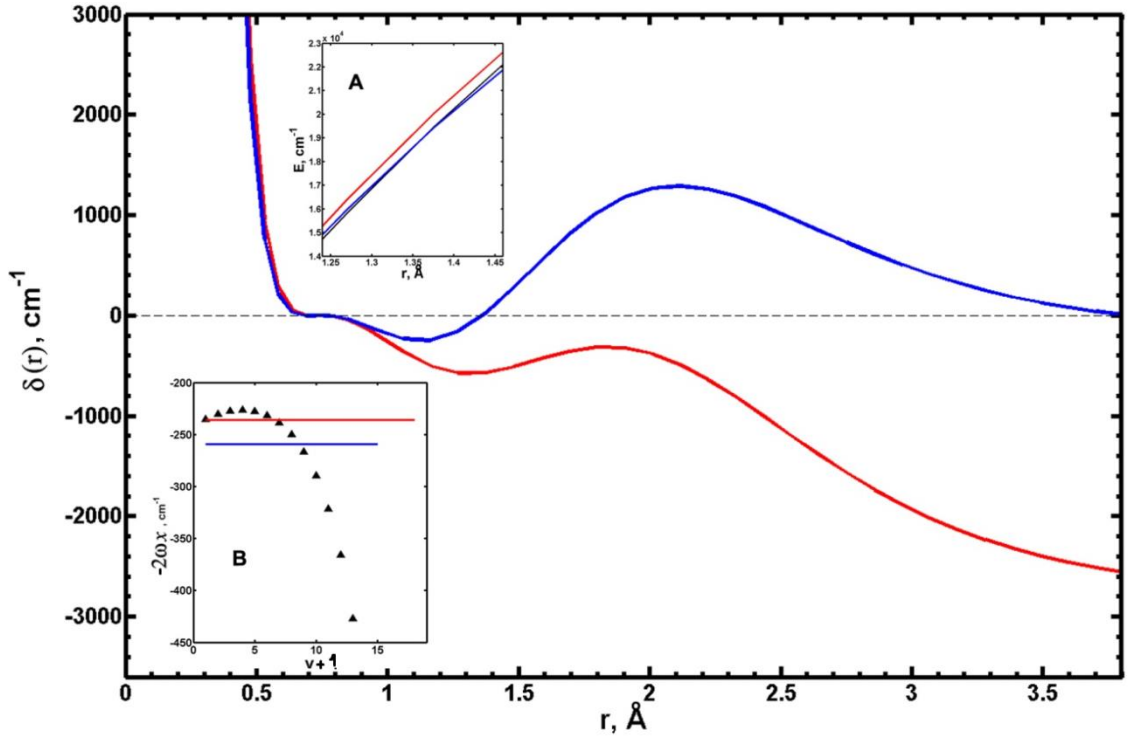

Figure 4. Deviations $\delta(r)$ of M1 (red line) and M2 (blue) from the term $X\ ^1\Sigma_g^+$ of hydrogen molecule H_2, according to [10]. Insert A shows a fragment of potential curves with the intersection of the M2 approximation with the $U(r)$ curve. Inset B - comparison of actual anharmonicity $\omega_e x(v)$ (triangles) and calculated constants $-2\omega_e x_e$ for M1 (red line) and $-2\omega_e x_e'$ for M2 (blue line)

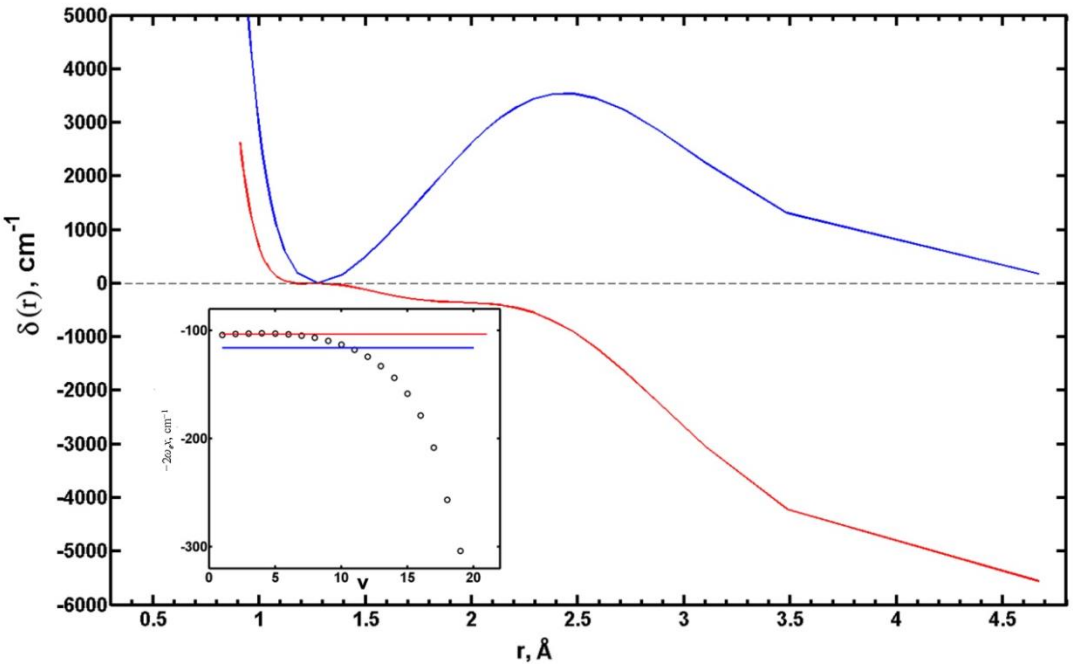

Figure 5. Deviations $\delta(r)$ for M1 (red line) and M2 (blue) from the term X $^2\Sigma^+$ of the HCl molecule according to [13]. Inset – the anharmonicity functions $-2\omega_e x(v)$ (points) and calculated values $-2\omega_e x_e$ for M1 (red line) and $-2\omega_e x'_e$ for M2 (blue line).

monotonously, forming at first a small minimum (small HA), and the deviation of M1 has a part almost parallel to the abscissa, where an inflection point is seen. Such are the terms X $^2\Sigma^+$ of the HCl molecule shown in Fig.5, and X $^3\Sigma_g^-$ of the O_2 molecule (see Fig.6). It is expedient to refer them to an intermediate type, transitional from a simple term to a term with a non-monotonous deviation function for M1. Although there is no clear minimum on the M1 curve, there are two parts with a change of the sign of the curvature between them at the inflection points at ~2.0 Å.

The presence of such parts significantly widens the interval in which the deviation of $\delta(r)$ is not large, and the M1 model better reproduces the real term. This pattern is well pronounced in the HA region of hydrogen. Although the deviation $\delta(r)$ for hydrogen in this part is not monotonous, its average value in a range of 0.7–2.2 Å (up to v=9, approximately 65% of the well depth) is about 400 cm^{-1}. This reduces the deviation D'_e from the real term to 7%. For HCl, the deviation rapidly increases to 5500 cm^{-1}, the extrapolated value of D'_e is ~15% higher than the real value 37232 cm^{-1}. The HCl molecule was several times used by the authors of textbooks and monographs to illustrate the accuracy of the estimate of the Morse dissociation energy (M1), the results do not differ significantly (17%, 15%, 20%). Other hydrogen halide molecules also likely belong to this group [2].

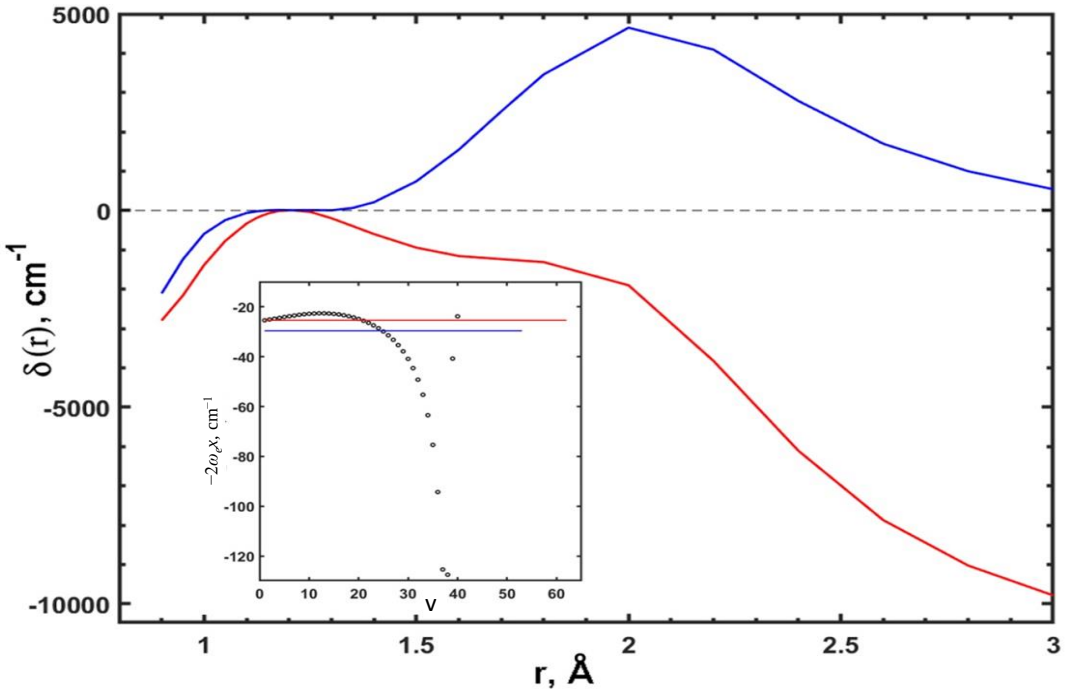

Figure 6. Deviations $\delta(r)$ for M1 (red line) and M2 (blue) from the term X $^3\Sigma_g^-$ of the O_2 molecule according to [14]. Inset - the anharmonicity function $-2\omega_e x(v)$ (points) and calculated values $-2\omega_e x_e$ for M1 (red) and $-2\omega_e x'_e$ for M2 (blue).

3.3. Peculiarities near asymptote

The third group includes O_2, Li_2, B_2, N_2 molecules, in which, in the upper part of the potential well of the ground state, when approaching the asymptote, a sharp decrease of anharmonicity is observed. In this section of the Birge-Sponer diagram, the shape of the curve noticeably changes, a concavity is formed (see Figs. 3 and 6 in [1]). The review by Le Roy [15] in Fig.6.4 shows two types of the Birge-Sponer diagram when approaching the asymptote, either convex, as in Fig.3 (points), with a tendency to intersect with the abscissa axis, or concave, as in the inset in Fig.9. This feature reflects the nature of the interatomic interaction at large amplitude of vibrations, where the second type is typical for the van der Waals interactions when they become dominant.

As an example, this feature is shown in Fig.6 in the inset for the ground term of the oxygen molecule. In addition to the features characteristic of a small HA in the lower part of the potential well, mentioned above, an anomalous, more than five-fold, decrease in anharmonicity occurs near the asymptote. It was shown in [1] on several examples that the anharmonicity $\omega_e x(v)$ of van der Waals molecules decreases monotonously over the entire range of quantum numbers v. It can be assumed that the anomaly near asymptote is caused by a change in the type of bond, the dominance of the van der Waals interaction upon strong excitation of molecular vibrations.

This anomaly creates difficulties in modeling of the spectra of strongly vibrationally exited molecules and of van der Waals molecules due to the different asymptotic of the Morse function (exponential) and the van der Waals interaction (inverse power series $\sum C_n/r^n$) requiring selection of the series coefficients for specific cases. The available data show that the anharmonicity of van der Waals molecules often decreases according to a more complex than linear law, and this provides useful auxiliary experimental data for modeling or correcting the interaction potential of diatomic molecules at a large interatomic distance before dissociation.

3.4. Ground terms of van der Waals molecules

For van der Waals molecules, as yet not numerous precise experimental spectra with complete vibrational structure are of particular value. An important example is the X $^1\Sigma^+$ term of the MgCa molecule with not a simple anharmonicity function; its functions $\delta(r)$ and $2\omega_e x(v)$ obtained from the fluorescence spectra [16] are shown in Fig.7. Since the value of $2\omega_e x(v)$ decreases throughout the succession of 22 vibrational levels, the value of the M1 function decreases during the approximation, and the $\delta(r)$ curve for M1 is located in the positive part. Curve M2 displays a characteristic distortion of the shape $U(r)$ and has also the opposite sign (compare the position of the horizontal lines in the inset), but the shape of

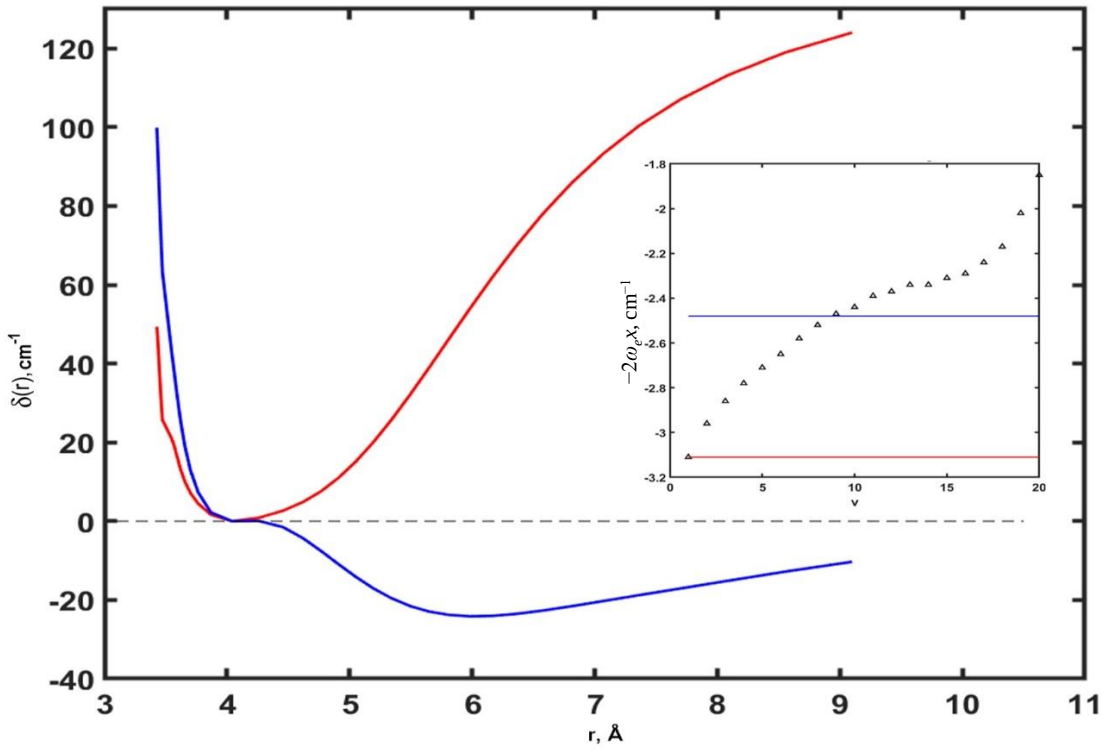

Figure 7. Deviations $\delta(r)$ of M1 (red line) and M2 (blue) from the term X $^1\Sigma^+$ of MgCa molecule constructed from experimental data [16]. Inset –the anharmonicity function $-2\omega_e x(v)$ $U(r)$ (triangles) and calculated values $-2\omega_e x_e$ for M1 (red line) and $-2\omega_e x'_e$ for M2 (blue line)

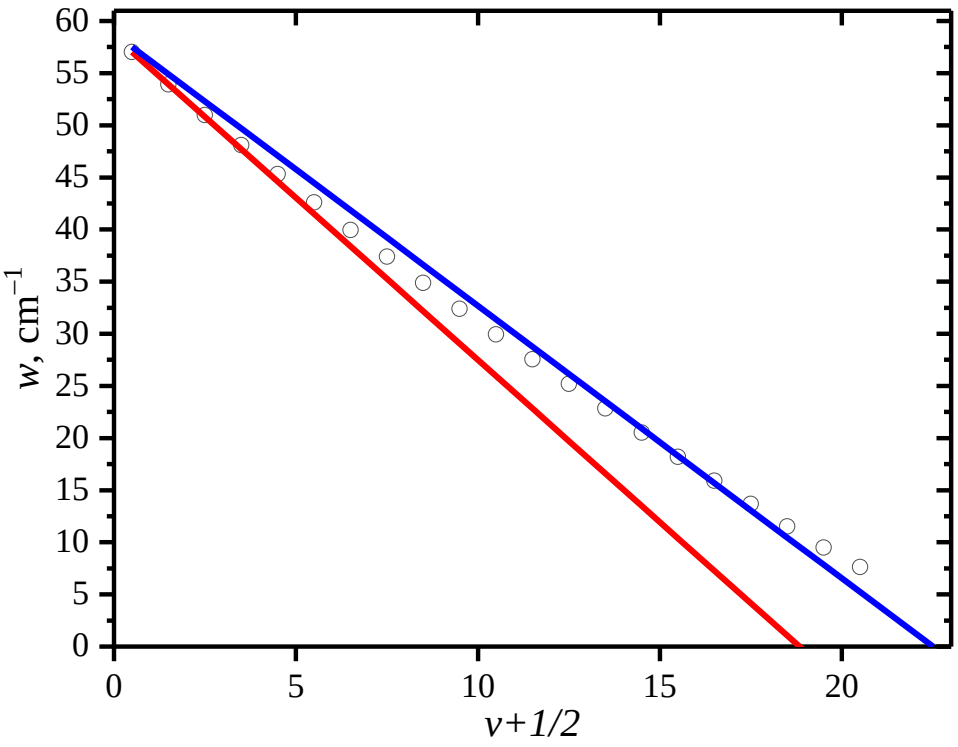

Figure 8. Birge-Sponer plot for the term $X\ ^1\Sigma^+$ of MgCa (points) according to the data from [16] and corresponding M1 (red line) and M2 (blue line) approximations.

anharmonicity function is of most importance here. The inset shows that in the lower half of the potential well, the anharmonicity decreases with deceleration (convex shape), and after the inflection point at $v = 13 - 14$, it decreases with acceleration (concave shape). These features reflect the specifics of van der Waals interactions and characterize the details of the shape of the term of van der Waals molecules. Only a slight concavity can be seen on the Birge-Sponer plot built using the same data (Fig. 8).

The anharmonicity function for the Si^+Ar complex (Fig. 9), constructed according to the data from [17], looks similar, only the signs of curvature are opposite, in the lower part of the well it is concave, and in the upper part it is convex. The inflection point is at v =11-12. At the same time, the Birge-Sponer plot almost does not differ from Fig.8. (see inset Fig.9).

Davies et al. [17] calculated the potential curves of the ground and excited states of twenty charged complexes of Si^+ and Ge^+ cations with noble gas atoms from He to Rn and plotted Birge-Sponer diagrams characterizing their vibrational structures. That article reported the frequencies of only two complexes, one of which is used to construct the anharmonicity function shown in Fig.9. Over the entire energy interval, the anharmonicity decreases, and in the upper part of the potential well it gradually approaches zero. It seems that the decrease of anharmonicity $|\omega_e x(v)|$ of molecular vibrations can serve as an empirical sign of van der Waals interactions. A concave shape is observed in the lower part of the well, which is not seen in the

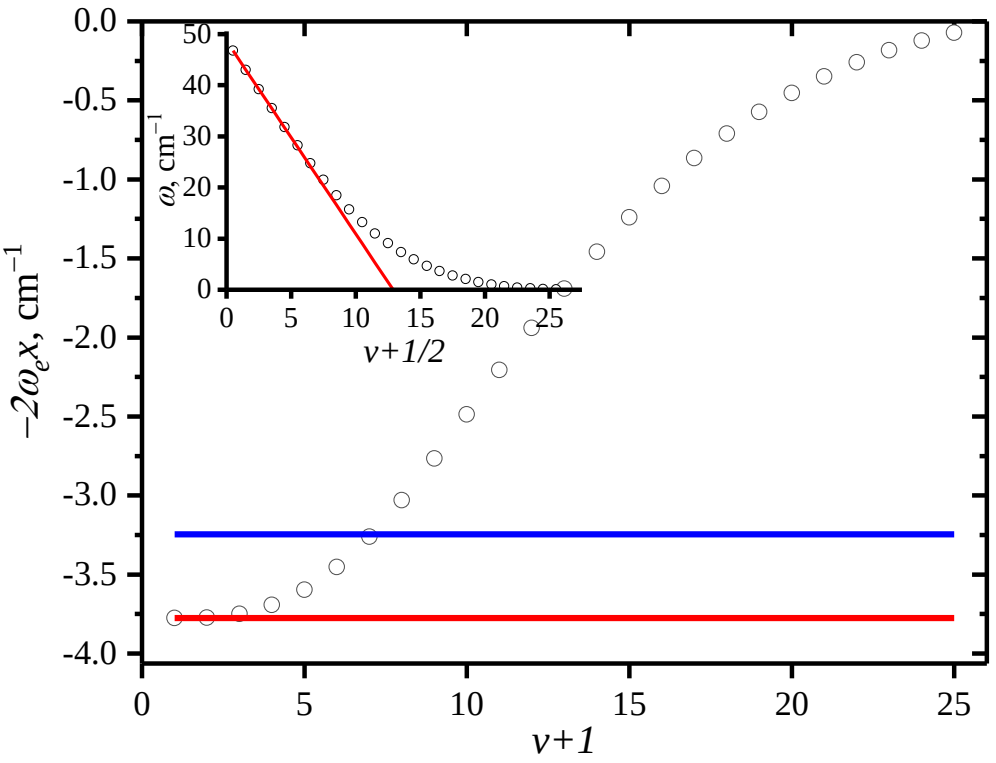

Figure 9. Anharmonicity function for the term $^2\Sigma^+$ for the $^{28}Si^+Ar$ complex (circles) according to [17] and corresponding constant values for M1 (red) and M2 (blue). The inset shows the Birge-Sponer plot for this term (circles), the M1 approximation $-2\omega_e x_e$ (red straight line), and for M2 approximation $-2\omega_e x'_e$ (blue)

Birge-Sponer diagram. Unfortunately, there are no spectra of such complexes in the literature that would make possible the assessment of the level of the theory used.

4. Conclusions

We described the basics of the methods for approximating the electronic term of a diatomic molecule $U(r)$ by the Morse function M(r), the simplest model of a real term with a single constant anharmonicity coefficient $\omega_e x_e$. The existence of two alternative approximations M1 and M2 is explained by the requirement to specify the bond energy D_e for a full description of a particular term, which Morse gives as $D_e = \omega_e^2/4\omega_e x_e$ (equation (15) in [4]). The distortion of the vibrational structure in the approximation is clearly illustrated in the Birge-Sponer coordinates $w(v) \equiv \Delta_1 G(v) = G(v+1) - G(v)$, where $w(v)$ (v=0,1,2,…v_m) is a sequence of vibrational quanta. We introduced the empirical anharmonicity function $\omega_e x(v)$ as a set of energy differences between neighboring vibrational quanta $\Delta\omega(v) \equiv \omega(v+1) - \omega(v) = -2\omega_e x(v)$ which provides a more precise characteristic of frequency deviations from a linear approximation and can serve as an individual characteristic of the term $U(r)$, useful for classifying the electronic terms of molecules. The function $\omega_e x(v)$ can be formally considered as the third approximation after ω_e (harmonic approximation, $x = 0$) and ω_e, $\omega_e x_e = C$ (the

simplest anharmonic approximation). In terms of the shape of the potential curve this will correspond to parabola with one constant (ω_e), Morse contour with two constants (ω_e, $\omega_e x_e$, or $\omega_e x_e'$), and the real molecule with the set (ω_e, $\omega_e x(v)$ and $\delta(r)$).

We introduced the function $\delta(r) \equiv U(r) - M(r)$, which quantitatively represents the changes of the shape of the contour of a real term during approximation. For many of the terms, the deviation $\delta(r)$ for M1 is negative (term M1 is located above $U(r)$ without crossing) and increases in absolute value with increasing r. For M2, the function $\delta(r)$ is usually positive, it has a domed shape, and approaches the abscissa at large r.

A particular type of deviation from the Morse model is found, which is manifested in either narrowing or broadening of the term in the lower part of the potential well and results in a decrease (or increase) in anharmonicity in some part of it (Herzberg Anomaly). In this case, the deviations $\delta(r)$ for M1 and M2 become more complicated and the terms $U(r)$ and M2 may intersect. Another particular type of deviation consists in a sharp decrease in the anharmonicity with increasing v near the asymptote. This jump is due to change of the law of interatomic attractions at large distances where the van der Waals interactions are predominant. By type of the shape of the anharmonicity function $\omega_e x(v)$ and deviations $\delta(r)$, we propose to divide the real terms of molecules with a valence bond into three groups: simple terms with monotonously increasing anharmonicity, terms with non-monotonous anharmonicity changes in the lower part of the potential well, and terms with a sharp decrease in anharmonicity near asymptotes.

A special group is presented by the set of van der Waals molecules, in which the anharmonicity decreases over the entire depth of the potential well, sometimes following a complex law. Here, of particular value are precise experimental data on the interatomic vibration frequencies, which can greatly facilitate the search for a theoretical model for describing a real term.

Systematic errors of approximation are due to the roughness of the constant anharmonicity model. In particular the overestimated value of the bond energy for M1, which is caused by imprecision of the equation (4), which is correct only for the Morse oscillator, i.e. for the exact equation (2). Similarly, for the M2 model, for which D_e is fixed, the change in the anharmonicity coefficient, carried out due to the factor x_e' , is realized using equation (4), which significantly changes the entire system of vibrational levels and leads to a significant broadening of the potential well. As a result, it turns out that the deviation $\delta(r)$ for M2 is smaller than for M1 only in small parts of the potential well, which include the minimum and the section adjacent to the asymptote. The inevitable result of the approximation is the appearance of fictitious vibrational levels adjacent to the asymptote from above for M1 and from below for M2.

These conclusions are based on a limited amount of experimental data, the extension to the more diverse molecules can make the picture more complex and necessitate more additions and possible changes.

Acknowledgments

The authors gratefully acknowledge valuable discussions and advices from Professors V.P. Bulychev, I.G. Denisov, H.-H. Limbach, I.G. Shenderovich.

REFERENCES

[1] G.S. Denisov, I.G. Denisov, More about properties of Morse oscillator. Spectr. Acta A 2021, 262(12), 120111/9 doi.org/10.1016/j.saa.2021.120111

[2] G.S. Denisov, K.G. Tokhadze, Implementation of Morse potential for approximation of vibrational terms of diatomic molecules. Optics Spectr. 2022, 130(14), 2096-2102. DOI: 10.21883/EOS.2022.14.53993.2483-21.

[3] G.S. Denisov, Empirical criteria of the quality of Morse approximation of the electronic term of diatomic molecule. Optika i Spektroskopija 2022, 130(9), 1306–1315. DOI: 10.21883/OS.2022.09.53289.3590-22. (in Russ).

[4] P.M. Morse, Diatomic molecules according to the wave mechanics. II. Vibrational levels. Phys. Rev. 1929, 34(1), 57-64. DOI: 10.1103/PhysRev.34.57

[5] S. Quadeer, G.D. Santis, P. Stins, S.X. Xanteas, Vibrational levels of a generalized Morse potential. J. Chem. Phys. 2022, 157(14), 144104. Vibrational levels of a generalized Morse potential. DOI: 10.1063/5.0103433

[6] L. Bytautas, N. Matsunaga, T. Nagata, M.S. Gordon, K. Ruedenberg, Accurate ab initio potential energy curve of F_2. III. The vibration rotation spectrum. J. Chem. Phys. 2007, 127(20), 204313/19. DOI: 10.1063/1.2805392

[7] L. Lessinger, Morse oscillators, Birge-Sponer extrapolation, and the electronic absorption spectrum of I_2. J. Chem. Educ. 1994, 71(5), 388-391. DOI: 10.1021/ed071p388

[8] G. Herzberg, Molecular Spectra and Molecular Structure I. Diatomic Molecules. New York, 1939. Fig.48.

[9] A.G. Gaydon, Dissociation Energies and Spectra of Diatomic Molecules, Chapman & Hall, L. 1968. Fig 10, page 109.

[10] L. Wolniewicz, Relativistic energies of the ground state of the hydrogen molecule. J. Chem. Phys. 1993, 99(3), 1851–1868. DOI: 10.1063/1.465303

[11] G. Herzberg, L.L. Howe, The Lyman bands of molecular hydrogen. Can. J. Phys. 1959, 37(5), 636–659. DOI: 10.1139/p59-070

[12] J.M. Merritt, V.E. Bondybey, M.C. Heaven, Berillium dimer – caught in the act of bonding. Science 2009, 324(5934), 1548–1551. DOI: 10.1126/science.1174326

[13] J.A. Coxon, P.G. Hadjigeorgiou, Improved direct potential fit analyses for the ground electronic states of the hydrogen halides: HF/DF/TF, HCl/DCl/TCl, HBr/DBr/TBr and HI/DI/TI. J. Quant. Spectr. Rad. Trans. 2015, 151, 133–154. DOI: 10.1016/j.jqsrt.2014.08.028

[14] L. Bytautas, N. Matsunaga, K. Ruedenberg, Accurate ab initio potential energy curve of O_2. II. Core-valence correlations, relativistic contributions, and vibration-rotation spectrum. J. Chem. Phys. 2010, 132(7), 074307/15. DOI: 10.1063/1.3298376

[15] R.J. Le Roy, Determining Equilibrium Structures and Potential Energy Functions for Diatomic Molecules, in: J. Demaison, Boggs, J.E., Császár, A.G. (Ed.) Equilibrium molecular structures. From Spectroscopy to Quantum Chemistry, Taylor & Francis Group, Boca Raton, 2011, pp. 159-204. DOI: 10.1201/b10374

[16] H. Atmanspacher, H. Scheingraber, S.R. Vidal, Laser induced fluorescence of the MgCa molecule. J. Chem. Phys. 1985, 82(8), 3491-3501. DOI: 10.1063/1.448929

[17] A.R. Davies, A. Cranney, L.A. Viehland, T.G. Wright, Interactions of $Si^+(^2P_J)$ and $Ge^+(^2P_J)$ with rare gas atoms (He-Rn): interaction potentials, spectroscopy, and ion transport. Phys. Chem. Chem. Phys. 2022, 24(11), 7144-7163. DOI: 10.1039/D1CP05710C.